

ADATIME: A Benchmarking Suite for Domain Adaptation on Time Series Data

MOHAMED RAGAB* and EMADDELDEEN ELDELE*, Nanyang Technological University, Singapore

WEE LING TAN, Institute for Infocomm Research, A*STAR, Singapore

CHUAN-SHENG FOO, Institute for Infocomm Research, A*STAR, Singapore

ZHENGHUA CHEN, Institute for Infocomm Research, A*STAR, Singapore

MIN WU, Institute for Infocomm Research, A*STAR, Singapore

CHEE-KEONG KWOH, Nanyang Technological University, Singapore

XIAOLI LI, Institute for Infocomm Research, A*STAR, Singapore and Nanyang Technological University, Singapore

Unsupervised domain adaptation methods aim to generalize well on unlabeled test data that may have a different (shifted) distribution from the training data. Such methods are typically developed on image data, and their application to time series data is less explored. Existing works on time series domain adaptation suffer from inconsistencies in evaluation schemes, datasets, and backbone neural network architectures. Moreover, labeled target data are usually employed for model selection, which violates the fundamental assumption of unsupervised domain adaptation. To address these issues, we develop a benchmarking evaluation suite (ADATIME) to systematically and fairly evaluate different domain adaptation methods on time series data. Specifically, we standardize the backbone neural network architectures and benchmarking datasets, while also exploring more realistic model selection approaches that can work with no labeled data or just few labeled samples. Our evaluation includes adapting state-of-the-art visual domain adaptation methods to time series data in addition to the recent methods specifically developed for time series data. We conduct extensive experiments to evaluate 10 state-of-the-art methods on four representative datasets spanning 20 cross-domain scenarios. Our results suggest that with careful selection of hyper-parameters, visual domain adaptation methods are competitive with methods proposed for time series domain adaptation. In addition, we find that hyper-parameters could be selected based on realistic model selection approaches. Our work unveils practical insights for applying domain adaptation methods on time series data and builds a solid foundation for future works in the field. The code is available at github.com/emadeldeen24/AdaTime.

ACM Reference Format:

Mohamed Ragab, Emadeldeen Eldele, Wee Ling Tan, Chuan-Sheng Foo, Zhenghua Chen, Min Wu, Chee-Keong Kwoh, and Xiaoli Li. 2022. ADATIME: A Benchmarking Suite for Domain Adaptation on Time Series Data. 1, 1 (March 2022), 25 pages. <https://doi.org/XXXXXXX.XXXXXXX>

*Both authors contributed equally to this research.

Authors' addresses: Mohamed Ragab, mohamedr002@e.ntu.edu.sg; Emadeldeen Eldele, emad0002@ntu.edu.sg, Nanyang Technological University, 50 Nanyang Ave, Singapore, 639798; Wee Ling Tan, Institute for Infocomm Research, A*STAR, 1 Fusionopolis Way, Singapore, 138632, weeling.tan@eng.ox.ac.uk; Chuan-Sheng Foo, Institute for Infocomm Research, A*STAR, 1 Fusionopolis Way, Singapore, 138632, foo_chuan_sheng@i2r.a-star.edu.sg; Zhenghua Chen, Institute for Infocomm Research, A*STAR, 1 Fusionopolis Way, Singapore, 138632, chen0832@e.ntu.edu.sg; Min Wu, Institute for Infocomm Research, A*STAR, 1 Fusionopolis Way, Singapore, 138632, wumin@i2r.a-star.edu.sg; Chee-Keong Kwoh, Nanyang Technological University, 50 Nanyang Ave, Singapore, 639798, asckkwoh@ntu.edu.sg; Xiaoli Li, Institute for Infocomm Research, A*STAR, 1 Fusionopolis Way, Singapore, 138632 and Nanyang Technological University, 50 Nanyang Ave, Singapore, 639798, xlli@i2r.a-star.edu.sg.

Permission to make digital or hard copies of all or part of this work for personal or classroom use is granted without fee provided that copies are not made or distributed for profit or commercial advantage and that copies bear this notice and the full citation on the first page. Copyrights for components of this work owned by others than ACM must be honored. Abstracting with credit is permitted. To copy otherwise, or republish, to post on servers or to redistribute to lists, requires prior specific permission and/or a fee. Request permissions from permissions@acm.org.

© 2018 Association for Computing Machinery.

Manuscript submitted to ACM

Manuscript submitted to ACM

1

1 INTRODUCTION

Time series classification problem is predominant in many real-world applications including healthcare and manufacturing. Recently, deep learning has gained more attention in time series classification tasks. It aims to learn the temporal dynamics in the complex underlying data patterns, assuming access to a vast amount of labeled data [1, 2]. Yet, annotating time series data can be challenging and burdensome due to its complex nature that requires expert domain knowledge [3–7]. One way to reduce the labeling burden is to leverage annotated data (e.g., synthetic or public data) from a relevant domain (i.e., source domain) for the model’s training while testing the model on the domain of interest (i.e., target domain). However, the source and target domains may have distinct distributions, resulting in a significant domain shift that hinders the model performance on the target domain. Such problem commonly exists in many time series applications including human activity recognition (HAR) [3, 8] and sleep stage classification (SSC) tasks [9]. For instance, a model can be trained to identify the activity of one subject (i.e., source domain) and tested on data from another subject (i.e., target domain), leading to poor performance that caused by the domain shift problem.

Unsupervised Domain Adaptation (UDA) aims to transfer knowledge learned from a labeled source domain to an unseen target domain, tackling the domain shift problem. A considerable amount of literature has been proposed for UDA on visual applications [10–12]. One prevailing paradigm aims to minimize statistical distribution measures to mitigate the distribution shift problem between the source and target domains [13–17]. Another promising paradigm that has recently emerged leverages the adversarial training techniques to mitigate the domain gap [18–20], inspired by generative adversarial networks [21].

Recently, more attention has been paid to time series UDA (TS-UDA) [3, 8, 22, 23]. However, previous work on TS-UDA methods suffers from the following limitations. First, most of the existing algorithms are specialized to particular applications or domains [3, 24, 25]. Thus, there is a clear shortage of baseline methods when applying domain adaptation on time series data. Second, existing TS-UDA works lack consistent evaluation schemes including benchmark datasets, preprocessing, and backbone networks. For instance, methods using recurrent neural networks as a backbone network [26] have been compared against methods with convolutional neural network based backbone networks [8]. In addition to differences in backbones, training procedures can also vary between different algorithms in terms of the number of epochs, weight decay, and learning rate schedulers [26, 27], which results in an inconsistent evaluation of new algorithms. Last, most of the existing TS-UDA approaches often utilize labeled data from the target domain for model selection, violating the unsupervised assumption of UDA [8, 23], and providing an over-optimistic view of their real-world performance. The aforementioned issues can contribute to the performance, and the performance gain is mistakenly attributed to the proposed UDA method.

In this work, we develop a systematic evaluation suite (*ADATIME*) to tackle the aforementioned obstacles and remove all extraneous factors to ensure a fair evaluation of different UDA algorithms on time series data. In *ADATIME*, we include current TS-UDA methods and re-implemented various state-of-the-art visual UDA methods that can be adapted to time series data. To ensure a fair evaluation of these methods, we standardize backbone networks and training procedures, data preparation, and preprocessing to address the inconsistency in previous evaluation schemes. Then, to select the model hyper-parameters, we explore more realistic model selection strategies that do not require target labels. Therefore, the main contributions of this paper can be summarized as follows:

- We systematically and fairly evaluate existing UDA methods on time series data. To the best of our knowledge, this is the first work to benchmark different UDA methods on time series data.

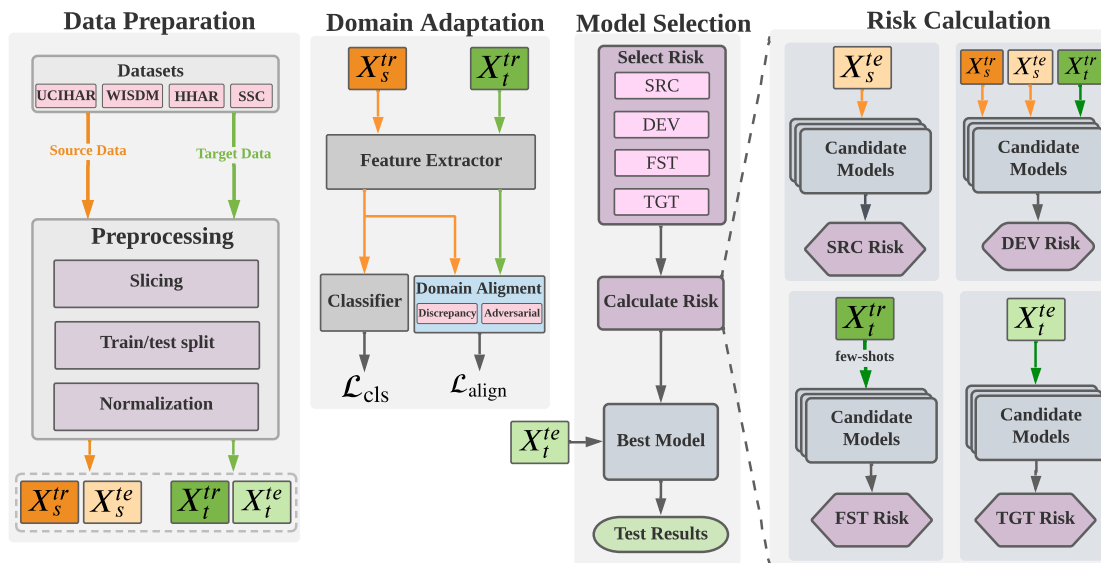


Fig. 1. Our benchmarking suite ADATIME consists of three main steps: Data Preparation, Domain Adaptation, and Model Selection. We first prepare the train and test data for both source and target domains (i.e., X_s^{tr} , X_s^{te} , X_t^{tr} , X_t^{te}). Then the training sets of source and target domains are passed through the backbone network to extract the corresponding features. The domain alignment algorithm being evaluated is then used to address the distribution shift between the two domains. Last, given a specific risk type, we calculate the risk value for all the candidate models and then, select the hyper-parameters of the one achieving the lowest risk. The selected model is lastly used for reporting the test results given the target domain test set (best viewed in color).

- We develop a benchmarking evaluation suite (ADATIME) that uses a standardized evaluation scheme and more realistic model selection techniques that align with UDA assumptions.
- We evaluate 10 state-of-the-art UDA methods on four representative time series datasets spanning 20 cross-domain scenarios, and presents comprehensive conclusions and recommendations for TS-UDA problem. These evaluation results and analysis can provide a systematic guideline for future research on TS-UDA.

The following sections are organized as follows. In Section 2, we define the unsupervised domain adaptation problem, and how adaptation is generally achieved. Section 3 describes the main components of our ADATIME suite such as benchmarking datasets, unified backbone networks, adapted UDA algorithms, model selection approaches and unified evaluation schemes. Section 4 shows the evaluation results and discusses the main findings of our experiments. Section 5 presents the main conclusions and recommendations.

2 DOMAIN ADAPTATION

2.1 Problem Formulation

We start by defining the unsupervised domain adaptation problem. We assume access to labeled data from a source domain $X_s = \{(x_s^i, y_s^i)\}_{i=1}^{N_s}$ that represents univariate or multivariate time series data, and unlabeled data from a target domain $X_t = \{(x_t^j)\}_{j=1}^{N_t}$, where N_s and N_t denote the number of samples for X_s and X_t respectively. Here we focus on classification and assume that both domains share the same label space $Y = \{1, 2, \dots, K\}$, where K is the number of

classes. Upon preprocessing, the source domain is split into a training set X_s^{tr} with N_s^{tr} samples, and a test set X_s^{te} with N_s^{te} samples. Similarly, the target domain is split into a training set X_t^{tr} with N_t^{tr} samples, and a test set X_t^{te} with N_t^{te} samples. The source and target domains are sampled from different marginal distributions, i.e., $P_s(x) \neq P_t(x)$, while the conditional distribution remains stable, i.e., $P_s(y|x) = P_t(y|x)$. The main goal of UDA is to minimize the distribution shift between $P_s(x)$ and $P_t(x)$, assuming they share the same label space.

2.2 General Approach

The mainstream of UDA algorithms is to address the domain shift problem by finding domain invariant feature representation. Formally, given a feature extractor network $f_\theta : X \rightarrow Z$, which transforms the input space to the feature space, the UDA algorithm mainly optimizes the feature extractor network to minimize a domain alignment loss $\mathcal{L}_{\text{align}}$, aiming to mitigate the distribution shift between the source and target domains such that $P_s(f_\theta(x)) = P_t(f_\theta(x))$. The domain alignment loss can either be estimated from a statistical distance measure or an adversarial discriminator network, which can be formalized as follows:

$$\mathcal{L}_{\text{align}} = \min_{f_\theta, h_\theta} \ell(Z_s, Z_t), \quad (1)$$

where ℓ can be a statistical distance or an adversarial loss.

Concurrently, a classifier network h_θ is applied on top of the feature extractor network to map the encoded features to the corresponding class probabilities. Particularly, given the source domain features Z_s generated from the feature extractor, we can calculate the output probabilities $\mathbf{p}_s = h_\theta(Z_s)$. Thus, the source classification loss can be formalized as follows

$$\mathcal{L}_{\text{cls}}^s = -\mathbb{E}_{(x_s, y_s) \sim P_s} \sum_{k=1}^K \mathbb{1}_{[y_s=k]} \log \mathbf{p}_s^k, \quad (2)$$

where $\mathbb{1}$ is the indicator function, which is set to be 1 when the condition is met, and set to 0 otherwise.

Both the source classification loss $\mathcal{L}_{\text{cls}}^s$ and the domain alignment loss $\mathcal{L}_{\text{align}}$ are jointly optimized to mitigate the domain shift while learning the source classification task, which can be expressed as

$$\min_{f_\theta, h_\theta} \mathcal{L}_{\text{cls}}^s + \mathcal{L}_{\text{align}}. \quad (3)$$

we refer to the composition of the the feature extractor f_θ and the classifier network h_θ as the model m , such that $m = h_\theta(f_\theta(\cdot))$.

3 ADATIME: A BENCHMARKING APPROACH FOR TIME SERIES DOMAIN ADAPTATION

3.1 Overview

In this work, we systematically evaluate different UDA algorithms on time series data, ensuring fair and realistic procedures. Fig. 1 shows the details of ADATIME flow, which proceeds as follows. Given a dataset, we first apply our standard data preparation schemes on both domains, including slicing, splitting to train/test portions, and normalization. Subsequently, the backbone network extracts the source and target features Z_s^{tr} and Z_t^{tr} from the the source training data X_s^{tr} and target training data X_t^{tr} respectively. The selected UDA algorithm is then applied to mitigate the distribution shift between the extracted features of the two domains. We generally categorize the adopted UDA algorithms into

discrepancy- and adversarial-based approaches. Last, to set the hyper-parameters of the UDA algorithm, we consider three practical model selection approaches that do not require any target domain labels or allow for only few-shot labeled samples. These approaches are source risk (SRC), deep embedded evaluation risk (DEV) [28], and few-shot target risk (FST). Our evaluation pipeline standardizes experimental procedures, preventing extraneous factors from affecting performance, thus enabling fair comparison between different UDA methods.

The code of ADATIME will be made publicly available for researchers to enable seamless evaluation of different UDA methods on time series data. Merging a new algorithm or dataset into ADATIME will be just a matter of adding a few lines of code.

3.2 Benchmarking Datasets

We select the most commonly used time series datasets from two real-world applications, i.e., human activity recognition and sleep stage classification. The benchmark datasets span a range of different characteristics including complexity, type of sensors, sample size, class distribution, and severity of domain shift, enabling more broad evaluation.

Table 1 summarizes the details of each dataset, e.g., the number of domains (D), the number of sensor channels (C), the number of classes (K), the length of each sample (L), as well as the total number of samples in both training and test portions. The selected datasets are detailed as follows:

3.2.1 UCIHAR. UCIHAR dataset [29] contains data from three sensors namely, accelerometer, gyroscope, and body sensors, that have been applied on 30 subjects. Each subject has performed six activities, i.e., walking, walking upstairs, downstairs, standing, sitting, and lying down. Due to the aforementioned variability between subjects, we treat each subject as a separate domain. Here, we randomly selected five cross-domain scenarios out of the large number of cross-domain combinations, as in [8, 23].

3.2.2 WISDM. In WISDM dataset [30], accelerometer sensors were applied to collect data from 36 subjects performing the same activities as in the UCIHAR dataset. However, this dataset can be more challenging because of the class-imbalance issue in the data of different subjects. Specifically, data from some subjects may contain only samples from a subset of the overall classes (see Fig. S.1 in the Appendix). Similar to the UCIHAR dataset, we consider each subject as a separate domain and randomly select five cross-domain scenarios.

3.2.3 HHAR. The Heterogeneity Human Activity Recognition (HHAR) dataset [31] has been collected from 9 different subjects using sensor readings from smartphones and smartwatches. In our experiments, we use the same smartphone device i.e., Samsung smartphone, for all the selected subjects to reduce the heterogeneity. In addition, we consider each subject as one domain and form the five cross-domain scenarios from randomly selected subjects.

3.2.4 SSC. Sleep stage classification (SSC) problem aims to classify the electroencephalography (EEG) signals into five stages i.e., Wake (W), Non-Rapid Eye Movement stages (N1, N2, N3), and Rapid Eye Movement (REM). We adopt Sleep-EDF dataset [32], which contains EEG readings from 20 healthy subjects. We select a single channel (i.e., Fpz-Cz) following previous studies [33], and include 10 different subjects to construct the five cross-domain scenarios.

3.3 Backbone Networks

In general, a UDA algorithm consists of a feature extractor network to extract the features from the input data, a classifier network to classify the features into different classes, and a domain alignment component to minimize the shift between domains. Here, we refer to feature extractor as the backbone network. The backbone network is responsible for

Table 1. Details of datasets. More details about selected cross-domain scenarios for each dataset can be found in Tables S.2, S.3, S.4, S.5 in the Appendix.

Dataset	D	C	K	L	Training set	Testing set
UCIHAR	32	9	6	128	2300	990
WISDM	36	3	6	128	1350	720
HHAR	9	3	6	128	12716	5218
SSC	20	1	5	3000	14280	6130

transforming the data from the input space to the feature space, where UDA algorithms are usually applied. Thus, the backbone network can have a significant influence on the performance of the UDA method, independent of the actual domain adaptation component. Hence, it is necessary to standardize the choice of backbone network to fairly compare between different UDA methods. However, some previous TS-UDA works adopted different backbone architectures when comparing against baseline methods, leading to inaccurate conclusions.

To tackle this problem, we design *ADATIME* to ensure the same backbone network is used when comparing between different UDA algorithms, promoting fair evaluation protocols. Furthermore, to better select a suitable backbone network for TS-UDA application, we experiment with three different backbone architectures: 1-dimensional convolutional neural network (1D-CNN), 1-dimensional residual network (1D-Resnet), and temporal convolutional neural network (TCN). These architectures are different in terms of their complexity and the number of trainable parameters. Note that these networks are widely used for time series data analytics [1, 4, 34–36].

Table 2. Summary of domain adaptation algorithms implemented in *ADATIME*

Algorithm	Application	Category	Distribution	Losses	Model Selection
DDC	Visual	Discrepancy	Marginal	MMD	Target Risk
Deep-Coral	Visual	Discrepancy	Marginal	CORAL	Not Mentioned
HoMM	Visual	Discrepancy	Marginal	High-order MMD	Not Mentioned
MMDA	Visual	Discrepancy	Joint	MMD, CORAL, Entropy	Target Risk
DSAN	Visual	Discrepancy	Joint	Local MMD	Not Mentioned
DANN	Visual	Adversarial	Marginal	Domain Classifier, Gradient Reversal Layer	Source Risk
CDAN	Visual	Adversarial	Joint	Conditional adversarial Domain Classifier	Importance Weighting
DIRT-T	Visual	Adversarial	Joint	Virtual adversarial Entropy Domain Classifier	Target Risk
CoDATS	Time Series	Adversarial	Marginal	Domain Classifier, Gradient Reversal Layer	Target Risk
AdvSKM	Time Series	Adversarial	Marginal	Spectral Kernel Adversarial MMD	Target Risk

3.4 Domain Adaptation Algorithms

While numerous UDA approaches have been proposed to address the domain shift problem [37], a comprehensive review of existing UDA methods is out of our scope. Besides including state-of-the-art methods proposed for time series data, we also included canonical methods for visual UDA that can be adapted to time-series. Overall, the implemented algorithms in ADATIME can be broadly classified according to the domain adaptation strategy, namely discrepancy-based methods and adversarial-based methods. The discrepancy-based methods aim to minimize a statistical distance between source and target features to mitigate the domain shift problem [13–15], while adversarial-based methods leverage a domain discriminator network that enforces the feature extractor to produce domain invariant features [38, 39]. Another way to classify UDA methods is based on what distribution is aligned distribution. Some algorithms only align the marginal distribution of the feature space [8, 13–15, 38, 40], while others jointly align the marginal and conditional distributions [16, 20, 41?], allowing fine-grained class alignment.

The selected UDA algorithms are as follows:

- **Deep Domain Confusion (DDC)** [15]: minimizes the Maximum Mean Discrepancy (MMD) distance between the source and target domains.
- **Correlation Alignment via Deep Neural Networks (Deep CORAL)** [42]: minimizes the domain shift by aligning second-order statistics of source and target distributions.
- **Higher-order Moment Matching (HoMM)** [14]: minimizes the discrepancy between different domains by matching higher-order moments of the source and target domains.
- **Minimum Discrepancy Estimation for Deep Domain Adaptation (MMDA)** [41]: combines both MMD and CORAL with conditional entropy minimization to address the domain shift.
- **Deep Subdomain Adaptation (DSAN)** [16]: minimizes the discrepancy between source and target domains via a local maximum mean discrepancy (LMMD) that aligns relevant subdomain distributions.
- **Domain-Adversarial Training of Neural Networks (DANN)** [38]: leverages gradient reversal layer to adversarially train a domain classifier against feature extractor network.
- **Conditional Adversarial Domain Adaptation (CDAN)** [20]: realizes a conditional adversarial alignment by incorporating the task knowledge with features during the domain alignment step.
- **A DIRT-T Approach to Unsupervised Domain Adaptation** [39]: employs virtual adversarial training, conditional entropy, and teacher model to align the source and target domains.
- **Convolutional deep Domain Adaptation model for Time Series data (CoDATS)** [8]: leverages adversarial training with weak supervision by a CNN network to improve the performance on time series data
- **Adversarial Spectral Kernel Matching (AdvSKM)** [23]: leverages adversarial spectral kernel matching to address the non-stationarity and non-monotonicity problem in time series data.

Table 2 summarizes the selected methods, showing the application for which each method was originally proposed, the classification of each method according to domain adaptation strategy (i.e., whether it relies on discrepancy measure or adversarial training), their classification based on the category of the aligned distribution (i.e., marginal or joint distribution), the losses in each method, and the risk that each UDA method adopted to tune its model hyper-parameters. It is worth noting that our ADATIME mainly focuses on time series classification problem, and hence we excluded methods proposed for time series prediction/forecasting.

3.5 Model Selection Approaches

Model selection and hyper-parameter tuning are long-standing non-trivial problems in UDA due to the absence of target domain labels. Throughout the literature, we find that the experimental setup in works use target domain labels to select hyper-parameters, which violates the main assumption of UDA. This is further clarified in Table 2, where we find that five out of the 10 adopted UDA works use the target risk (i.e., target domain labels) in their experiments to select the hyper-parameters, while another three works use fixed hyper-parameters without describing how they are selected. To address this issue, we evaluate multiple realistic model selection approaches that do not require any target domain labels, such as: source risk [19] and Deep Embedded Validation (DEV) risk [28]. In addition, we design a few-shot target risk that utilizes affordable few labeled samples from the target domain. In the following subsections, we explain the risk calculation for each model selection approach.

3.5.1 Selection of Best Model. As shown in Fig. 1, given a set of n candidate models $\mathcal{M} = (m_1, m_2, \dots, m_n)$ with different hyper-parameters. First, we calculate the corresponding risk value for each candidate model with respect to each model selection approach. Subsequently, we rank candidate models based on their computed risk while selecting the model with minimum risk value.

$$m_{best} = \min_{m \in \mathcal{M}} \mathcal{R}_*(m), \quad (4)$$

where m_{best} is the best model that achieves the minimum risk value, and $\mathcal{R}_* \in \{\mathcal{R}_{SRC}, \mathcal{R}_{DEV}, \mathcal{R}_{FST}, \mathcal{R}_{TGT}\}$ can be any of the model selection approaches described below.

3.5.2 Source Risk (SRC). In this approach, we select the candidate model that achieves the minimum cross-entropy loss on a test set from the source domain. Therefore, this risk can be easily applied without any additional labeling effort as it relies on existing labels from the source domain [19]. Given the source domain test data (x_s^{te}, y_s^{te}) , and a candidate model m , we calculate the corresponding source risk \mathcal{R}_{SRC} as:

$$\mathcal{R}_{SRC}(m) = \mathbb{E}_{x_s \sim P_s(x)} \ell_{ce}(m(x_s^{te}), y_s^{te}), \quad (5)$$

where ℓ_{ce} is the cross-entropy loss. Despite the simplicity of the source risk, its effectiveness is mainly influenced by the sample size of source data and the severity of the distribution shift.

3.5.3 DEV Risk. This approach [28] aims to find an unbiased estimator of the target risk. The key idea is to consider the correlation between the source and target features during the risk calculation. More specifically, the DEV method aims to emphasize source features that are highly correlated to the target features while giving lower weights to the less correlated features. To do so, an importance weighting scheme has been applied on the feature space. Given the source domain training features Z_s^{tr} , the source domain test set Z_s^{te} , and the target domain training features Z_t^{tr} , we first train a two-layer logistic regression model r_θ to discriminate between Z_s^{tr} and Z_t^{tr} (label features from Z_s^{tr} as 1, and Z_t^{tr} as 0), which can be formalized as follows

$$\min_{r_\theta} \mathcal{L}_d = [\log r_\theta(Z_s^{tr}) + \log(1 - r_\theta(Z_t^{tr}))]. \quad (6)$$

Subsequently, we leverage the trained r_θ to compute the importance weights w_f for the source test set as follows.

$$w_f(x_s^{te}) = \frac{N_s^{tr}}{N_t^{tr}} \frac{1 - r_\theta(Z_s^{te})}{r_\theta(Z_s^{te})}, \quad (7)$$

where $\frac{N_s^{tr}}{N_t^{tr}}$ is sample size ratio of both domains. Given the importance weights for each test sample of the source domain, we compute the corresponding weighted cross-entropy loss, L_w , for the test samples of the source domain, which can be expressed as

$$L_w = \{w_f(x_s^{te})\ell_{ce}(m(x_s^{te}), y_s^{te})\}_i^{N_s^{te}}, \quad (8)$$

where m is one candidate model. Given the weighted source loss L_w and its corresponding importance weight $W = \{w_f(x_s^{te})\}$, we compute the DEV risk as follows:

$$\mathcal{R}_{DEV} = \text{mean}(L_w) + \eta \text{mean}(W) - \eta, \quad (9)$$

where $\eta = -\frac{\text{Cov}(L_w)}{\text{Var}(W)}$ is the optimal coefficient. The DEV risk can be more effective than the source risk. However, we observed in our experiments that DEV may have unstable performance with smaller source and target datasets and adds additional computational overheads.

3.5.4 Target Risk (TGT). This approach involves leaving out a large subset of target domain samples and their labels as a validation set, and using them to select the best candidate model. Using this risk naturally yields the best performing hyper-parameters on the target domain. This can be seen as the upper bound for the performance of a UDA method. The target risk \mathcal{R}_{TGT} is calculated as:

$$\mathcal{R}_{TGT} = \mathbb{E}_{x_t \sim P_t(x)} \ell_{ce}(m(x_t^{te}), y_t^{te}). \quad (10)$$

Even though this approach is impractical in unsupervised settings, it has been used for model selection in many previous UDA papers [39, 43].

3.5.5 Few-Shot Target (FST) Risk. We propose few-shot target risk as a more practical alternative to the target risk. While labeling large amounts of time series data can be laborious, annotating a few samples per class can still be affordable and realistic in many real-world applications. Here, we use a set of q samples from the target domain as a validation set to select the best candidate model. The few-shot target risk \mathcal{R}_{FST} is calculated as follows.

$$\mathcal{R}_{FST} = \frac{1}{q} \sum_{i=1}^q \ell_{ce}(m(x_t^i), y_t^i). \quad (11)$$

We observe in our experiments that this strategy can achieve very close performance to the over-optimistic target risk, despite being computed with only a few samples.

3.6 Standardized Evaluation Scheme

3.6.1 Standardized Data Preprocessing. The preprocessing of time series data includes data slicing, train/test splitting, and normalization. To enable fair evaluation, we ensured consistent pre-processing when comparing different UDA algorithms. We use a sliding window of 128 for human activity recognition datasets, while we keep the original sample length of 3,000 time steps in the SSC dataset. Next, we split both source and target domains into train/test splits with a ratio of 0.7/0.3. Finally, we normalize both training and testing data based on the training statistics [8, 23]. For the WISDM dataset, we select the domains from subjects that contain samples from all the classes to stabilize the training.

3.6.2 Standardized Training Scheme. All the training procedures have been standardized across all UDA algorithms. For instance, we train each model for 40 epochs, as performance tends to decrease with longer training. We report the

model performance after the end of the last epoch. For model optimization, we use Adam optimizer with a fixed weight decay of $1e-4$ and $(\beta_1, \beta_2) = (0.5, 0.99)$. The learning rate is set to be a tuneable hyper-parameter for each method on each dataset. We exclude any learning rate scheduling schemes from our experiments to ensure that the contribution is mainly attributed to the UDA algorithm.

3.6.3 Hyper-parameter Search. For each algorithm/dataset combination, we conduct an extensive random hyper-parameter search with 100 hyper-parameter combinations. The hyper-parameters are picked by a uniform sampling from a range of predefined values. Details about the specified ranges can be found in Table S.1 of the Appendix. For each set of hyper-parameters, we calculate the values of the four risks for three different random seeds. We pick the model that achieves the minimum risk value for each model selection strategy. To calculate the FST risk, we use five samples per class from each dataset.

3.6.4 Evaluation Metric. Since time series data are usually imbalanced, where some classes might be totally absent from some subjects (see Fig. S.1b in the Appendix), the accuracy metric may not be representative of the performance of the UDA methods. Therefore, we report macro F1-scores instead, which take into account how the data is distributed, and avoids predicting false negatives.

4 RESULTS AND DISCUSSIONS

In this section, we first investigate the contributions of different backbone networks to the performance of UDA algorithms. Subsequently, we study the performance of different model selection techniques on the benchmark datasets. Last, we discuss the main findings of our experiments.

4.1 Evaluation of Backbone Networks

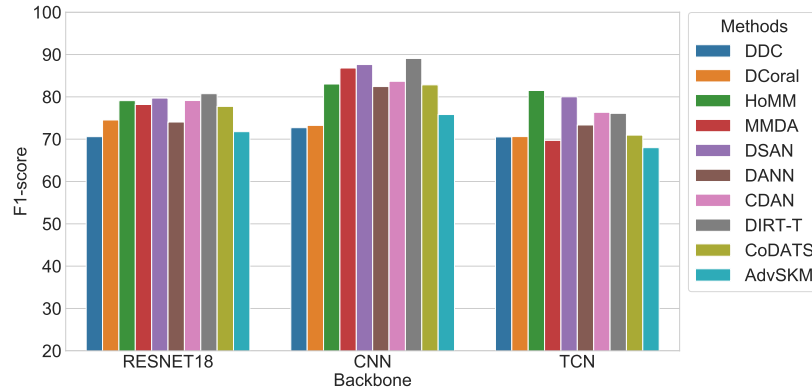
To investigate the impact of the backbone networks on the models' performance, we evaluate all the UDA algorithms under three different backbone networks. Particularly, we employ 1D-CNN, 1D-ResNet-18, and TCN (described in Section 3.3) as backbone networks. To better evaluate the performance of different backbone networks, we experimented on datasets with different scales. Specifically, we selected a small scale dataset such as UCIHAR, and a large-scale dataset such as HHAR. We reported the average performance of all cross-domain scenarios in the adopted datasets, as shown in Fig. 2. Clearly, the absolute performance varies significantly across different backbone networks for the same UDA method. Nonetheless, the relative performance between different UDA methods remains stable across the three backbone networks. For instance, while DIRT-T consistently performs best, DDC has the lowest performance with respect to all the other UDA methods, independently of the utilized backbone networks. On the other hand, comparing performance of different backbone networks suggests that the simple 1D-CNN network can consistently outperform more complex backbone networks, i.e., 1D-Resnet-18, and TCN. A possible explanation is that time series data has lower dimensionality, and hence, more complex backbone networks can be more prone to the overfitting problem that degrades the cross-domain performance [1].

4.2 Evaluation of Model Selection Strategies

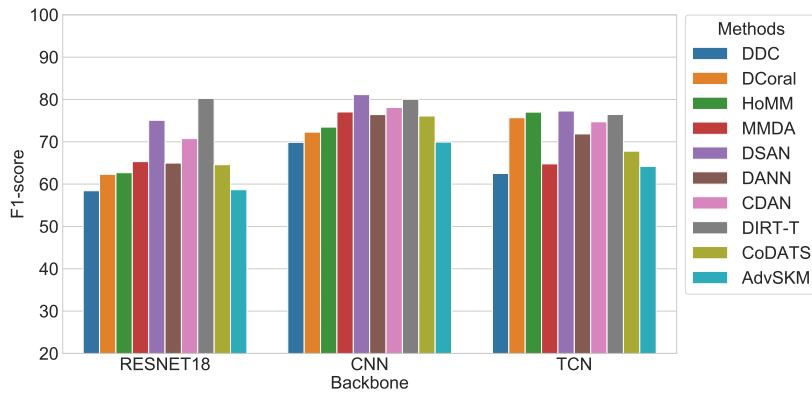
In the experiment, we evaluate the performance of different risks i.e., SRC, DEV, FST, and TGT (described in Section 3.5) on the UDA methods. To do so, we first fix the backbone network to be 1D-CNN due to its stable performance and computational efficiency. Then, for all the UDA algorithms, we select the best model according to each model selection strategy while testing its performance on the target domain data. Table 3 shows the average F1-score performance

Table 3. The average results (from 5 cross-domain scenarios) according to the minimum risk value in terms of MF1-score applied on 1D-CNN backbone.

Dataset	Algorithm	SRC Risk	DEV Risk	FST Risk	TGT Risk
UCIHAR	DDC	68.83	74.14	74.25	75.67
	Deep-Coral	71.99	71.43	77.23	77.71
	HoMM	75.86	78.28	81.3	84.10
	MMDA	80.12	80.12	79.54	81.40
	DSAN	83.31	<u>81.07</u>	<u>87.13</u>	<u>90.96</u>
	DANN	79.82	<u>80.89</u>	83.1	84.97
	CDAN	<u>86.55</u>	64.66	86.79	86.79
	DIRT-T	86.72	82.54	88.47	92.20
	CoDATS	79.05	65.12	79.1	85.47
	AdvSKM	71.08	74.62	74.47	74.67
	Avg/risk	78.33	75.29	81.14	83.39
WISDM	DDC	54.98	52.80	50.05	55.03
	Deep-Coral	55.54	53.85	49.45	57.43
	HoMM	57.49	61.23	46.56	62.98
	MMDA	<u>57.53</u>	57.30	52.12	<u>63.97</u>
	DSAN	56.51	56.51	<u>53.41</u>	<u>60.08</u>
	DANN	53.21	54.48	49.45	57.81
	CDAN	52.49	53.27	52.75	57.85
	DIRT-T	60.43	53.24	62.61	66.28
	CoDATS	52.72	54.27	48.64	56.57
	AdvSKM	53.95	<u>57.46</u>	49.02	60.55
	Avg/risk	53.93	53.52	51.91	60.82
HHAR	Deep-Coral	70.78	69.88	70.68	72.28
	HoMM	71.18	72.50	68.62	73.47
	MMDA	66.20	70.23	71.07	77.04
	DSAN	76.18	78.95	<u>78.18</u>	81.14
	DANN	<u>76.24</u>	72.62	73.68	76.42
	CDAN	77.74	77.43	77.43	78.09
	DIRT-T	75.56	<u>78.69</u>	78.41	<u>80.04</u>
	CoDATS	75.11	73.72	74.74	76.09
	ADVSKM	66.58	66.96	69.93	69.93
	Avg/risk	72.32	72.73	73.20	75.44
SSC	DDC	59.18	59.21	59.22	59.22
	Deep-Coral	59.12	58.81	58.82	59.12
	HoMM	59.06	<u>60.95</u>	58.70	59.06
	MMDA	62.08	61.49	57.98	62.79
	DSAN	58.14	59.85	58.97	<u>60.57</u>
	DANN	<u>60.26</u>	57.77	60.26	60.26
	CDAN	<u>54.89</u>	56.86	56.17	59.04
	DIRT-T	58.44	59.26	58.23	59.42
	CoDATS	56.76	55.79	54.64	58.44
	AdvSKM	59.94	59.92	<u>59.93</u>	60.21
	Avg/risk	59.37	59.34	59.10	60.30



(a) UCIHAR dataset



(b) HHAR dataset

Fig. 2. Comparison between 1D-CNN, 1D-ResNet-18, TCN backbones applied on the both UCIHAR and HHAR datasets. Results are in terms of macro F1-score.

across all the cross-domain scenarios spanning four different datasets (detailed versions can be found in Tables S.2, S.3, S.4, S.5 in the Appendix.). Overall, model selection strategies have a strong influence on the final test performance of UDA algorithms. In addition, on all the four datasets, TGT risk performs best compared to the other model selection strategies as expected. However, the performance gaps between different model selection strategies becomes smaller with large-scale datasets. More specifically, for small-datasets, i.e., UCIHAR and WISDM, the target risk outperforms the second best model selection strategy by 2.25% and 6.89% respectively. In contrast, for large-scale datasets, i.e., SSC and HHAR, the performance gap diminishes to 0.93% and 2.24% respectively. To sum up, the efficacy of different model selection strategies increases with larger sample size. Furthermore, with affordable labeling efforts, our proposed few-shot target risk can also achieve a competitive performance to the target risk.

Table 4. Domain gap between the source and target domains described by the difference between lower and upper performance bounds of 1D-CNN backbone.

	HAR	HHAR	WISDM	SSC
Same Domain (Target-only)	100.00	98.76	98.01	73.73
Cross-Domain (Source-only)	62.68	64.90	48.57	55.35
Gap (δ)	37.32	33.86	49.44	18.38

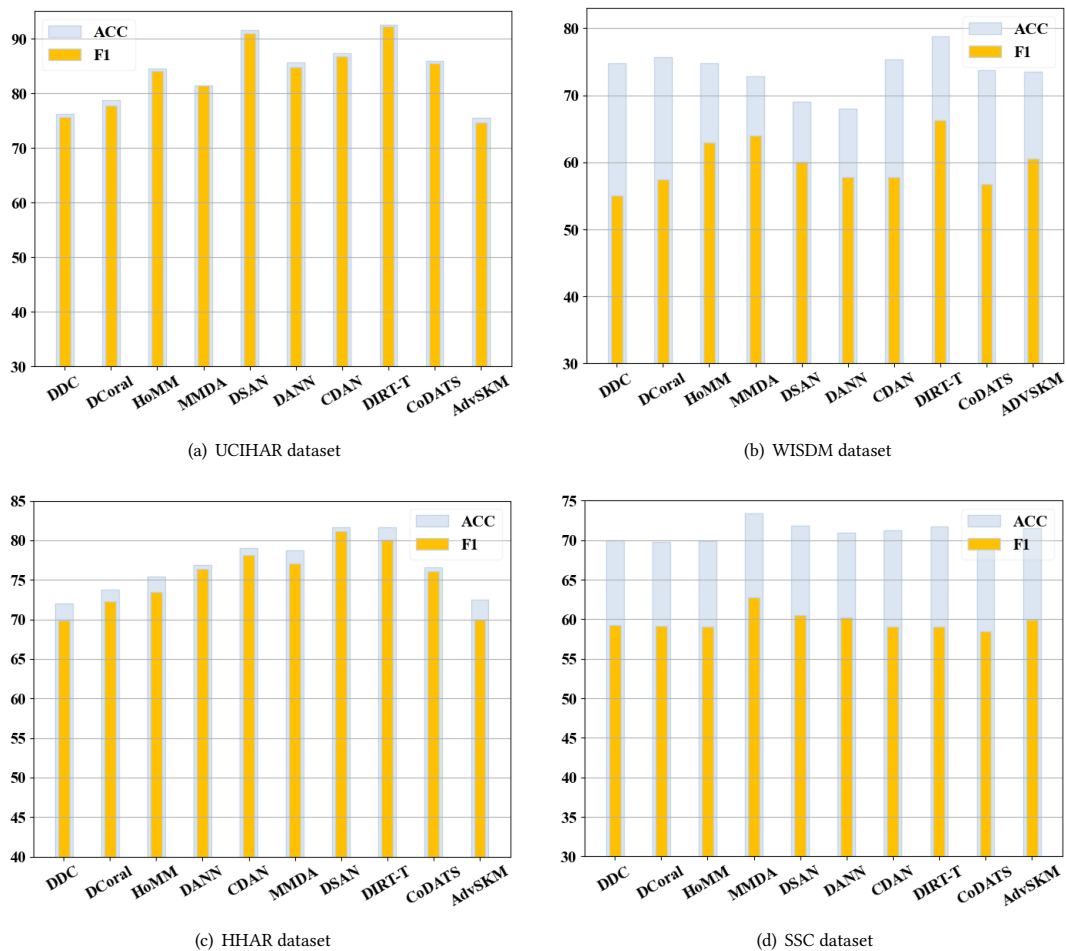


Fig. 3. Results of best models according to target risk for different methods in terms of accuracy and macro average F1-score.

4.3 Discussions

ADATIME provides a unified framework to evaluate different UDA methods on time series data. To explore the advantage of one UDA method over the others, we fixed the backbone network, the evaluation schemes, and the model selection strategy. We unveil the following insights.

Domain gap of different datasets. We conducted the experiments on two small-scale datasets, and two large-scale datasets. Regardless of the dataset size, all the adopted datasets suffer a considerable domain gap, as shown in Table 4. This table provides the results of target-only experiment (i.e., training the model with target domain training set and testing it directly on the target domain test set), and the source-only experiment (i.e., training the model with source domain training set and testing it directly on the target domain test set). The backbone network for both experiments is 1D-CNN network. While the source-only represents the lower-bound performance, the target only represents the upper bound performance, and the domain gap is represented by their difference.

Visual UDA methods achieve comparable performance to TS-UDA methods on time series data. With further exploration to Table 3, we find that surprisingly the performance of visual UDA methods is competitive or even better than TS-UDA methods. This finding is consistent for all the model selection strategies across the benchmarking datasets. For example, with the TGT risk value, we find that the methods proposed for visual applications such as DIRT-T and DSAN perform better than CoDATS and AdvSKM on the four datasets. A possible explanation is that all the selected UDA algorithms are applied on the vectorized feature space generated by the backbone network, which is independent of the input data modality. This finding suggests that with a standard backbone network, visual UDA algorithms can be strong baselines for TS-UDA.

Methods with joint distribution alignment tend to perform consistently better. Table 2 illustrates that some methods address the marginal distribution such as MMD, CORAL and HoMM, while the others address the joint distributions (i.e., both marginal and conditional distributions concurrently) such as DIRT-T, MMDA, and DSAN. The results shown in Table 3 suggest that the methods addressing the joint distribution outperform those addressing the marginal distribution. For example, the best performing method, as selected by the TGT risk, is DIRT-T in both UCIHAR and WISDM datasets, and DSAN in both SSC and HHAR datasets. Similarly, with respect to different risks, DIRT-T, MMDA, and DSAN interchangeably achieve the best performance across the benchmarking datasets. Hence, considering the conditional distribution when designing the UDA algorithm is beneficial to the performance.

Accuracy metric should not be used to measure performance for imbalanced data. While it is well-known that accuracy is not a representative metric for class-imbalanced datasets, existing TS-UDA methods are still using it to report their performance [3, 8, 23]. Throughout our experiments, we noticed that for imbalanced datasets such as WISDM, we usually have inconsistent results when adopting accuracy alone or F1-score alone. Therefore, we aim to re-emphasize that the accuracy metric gives over-optimistic results when considering the imbalanced nature in most of time series data. To further illustrate this, we provide the results in terms of both accuracy and F1-score on the four datasets, as shown in Fig. 3. It is worth noting that WISDM and SSC datasets are imbalanced, while UCIHAR and HHAR datasets are mostly balanced. Considering WISDM dataset in Fig. 3(b), we notice that although CDAN achieves higher accuracy than some other methods such as DDC, MMDA, and DSAN, it performs the worst in terms of F1-score. In contrast, the results of the balanced UCIHAR dataset in Fig. 3(a), reveal that accuracy can still be representative and indicate similar performance to F1-Score. Hence, we suggest to adopt the F1-score as a performance measure in all the experiments.

5 CONCLUSIONS AND RECOMMENDATIONS

In this work, we provided ADATIME, a systematic evaluation suite for evaluating existing domain adaptation methods on time series data. To ensure fair and realistic evaluation, we standardized the benchmarking datasets, evaluation schemes, and backbone networks among different domain adaptation methods. Moreover, we explored more realistic model selection approaches that can work without any target domain labels or with only few-shot labeled samples.

Based on our systematic study, we provide some recommendations as follows. First, visual UDA methods can be applied on time series data and are strong candidate baselines. Second, we can rely on more realistic model selection strategies, that do not require target domain labels such as source risk and DEV risk, to achieve reliable performance. Third, we recommend to conduct experiments with large-scale datasets to obtain reliable results, with fixing the backbone network among different UDA baselines. We also suggest to adopt F1-score instead of accuracy as a performance measure to avoid any misleading results with imbalanced datasets.

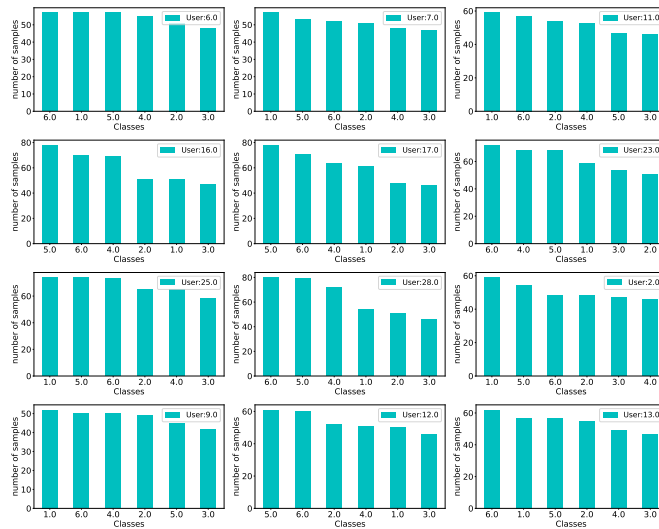
REFERENCES

- [1] Hassan Ismail Fawaz, Germain Forestier, Jonathan Weber, Lhassane Idoumghar, and Pierre-Alain Muller. Deep learning for time series classification: a review. *Data Mining and Knowledge Discovery*, 33(4):917–963, 2019.
- [2] Jason Lines, Sarah Taylor, and Anthony Bagnall. Time series classification with hive-cote: The hierarchical vote collective of transformation-based ensembles. *ACM Transactions on Knowledge Discovery from Data*, 12(5), 2018.
- [3] Youngjae Chang, Akhil Mathur, Anton Isopoussu, Junehwa Song, and Fahim Kawsar. A systematic study of unsupervised domain adaptation for robust human-activity recognition. *Proceedings of the ACM on Interactive, Mobile, Wearable and Ubiquitous Technologies*, 4(1):1–30, 2020.
- [4] Emadeldeen Eldele, Mohamed Ragab, Zhenghua Chen, Min Wu, Chee Keong Kwoh, Xiaoli Li, and Cuntai Guan. Time-series representation learning via temporal and contextual contrasting. In *Proceedings of the Thirtieth International Joint Conference on Artificial Intelligence, IJCAI-21*, pages 2352–2359, 2021.
- [5] Yangfan Li, Kenli Li, Cen Chen, Xu Zhou, Zeng Zeng, and Keqin Li. Modeling temporal patterns with dilated convolutions for time-series forecasting. *ACM Transactions on Knowledge Discovery from Data (TKDD)*, 16(1):1–22, 2021.
- [6] Yi Li, Yang Sun, Kirill Horoshenkov, and Syed Mohsen Naqvi. Domain adaptation and autoencoder-based unsupervised speech enhancement. *IEEE Transactions on Artificial Intelligence*, 3(1):43–52, 2021.
- [7] Arun Kumar Sharma and Nishchal K Verma. Quick learning mechanism with cross-domain adaptation for intelligent fault diagnosis. *IEEE Transactions on Artificial Intelligence*, 2021.
- [8] Garrett Wilson, Janardhan Rao Doppa, and Diane J. Cook. Multi-source deep domain adaptation with weak supervision for time-series sensor data. In *SIGKDD*, 2020.
- [9] Emadeldeen Eldele, Mohamed Ragab, Zhenghua Chen, Min Wu, Chee-Keong Kwoh, Xiaoli Li, and Cuntai Guan. Adast: Attentive cross-domain eeg-based sleep staging framework with iterative self-training, 2021.
- [10] Shuteng Niu, Yongxin Liu, Jian Wang, and Houbing Song. A decade survey of transfer learning (2010–2020). *IEEE Transactions on Artificial Intelligence*, 1(2):151–166, 2020.
- [11] Chaoyue Wang, Chang Xu, and Dacheng Tao. Self-supervised pose adaptation for cross-domain image animation. *IEEE Transactions on Artificial Intelligence*, 1(1):34–46, 2020.
- [12] Hanrui Wu and Michael K Ng. Multiple graphs and low-rank embedding for multi-source heterogeneous domain adaptation. *ACM Transactions on Knowledge Discovery from Data (TKDD)*, 16(4):1–25, 2022.
- [13] Baochen Sun and Kate Saenko. Deep coral: Correlation alignment for deep domain adaptation. In *ECCV*, pages 443–450. Springer, 2016.
- [14] Chao Chen, Zhihang Fu, Zhihong Chen, Sheng Jin, Zhaowei Cheng, Xinyu Jin, and Xian-Sheng Hua. Homm: Higher-order moment matching for unsupervised domain adaptation. *AAAI*, 2020.
- [15] Eric Tzeng, Judy Hoffman, Ning Zhang, Kate Saenko, and Trevor Darrell. Deep domain confusion: Maximizing for domain invariance. *arXiv preprint arXiv:1412.3474*, 2014.
- [16] Yongchun Zhu, Fuzhen Zhuang, Jindong Wang, Guolin Ke, Jingwu Chen, Jiang Bian, Hui Xiong, and Qing He. Deep subdomain adaptation network for image classification. *IEEE Transactions on Neural Networks and Learning Systems*, 32(4):1713–1722, 2021.
- [17] Erheng Zhong, Wei Fan, Jing Peng, Kun Zhang, Jiangtao Ren, Deepak Turaga, and Olivier Verscheure. Cross domain distribution adaptation via kernel mapping. In *Proceedings of the 15th ACM SIGKDD international conference on Knowledge discovery and data mining*, pages 1027–1036, 2009.
- [18] Mingsheng Long, Yue Cao, Jianmin Wang, and Michael Jordan. Learning transferable features with deep adaptation networks. In *International conference on machine learning*, pages 97–105. PMLR, 2015.
- [19] Yaroslav Ganin, Evgeniya Ustinova, Hana Ajakan, Pascal Germain, Hugo Larochelle, François Laviolette, Mario Marchand, and Victor Lempitsky. Domain-adversarial training of neural networks. *The Journal of Machine Learning Research*, 17(1):2096–2030, 2016.

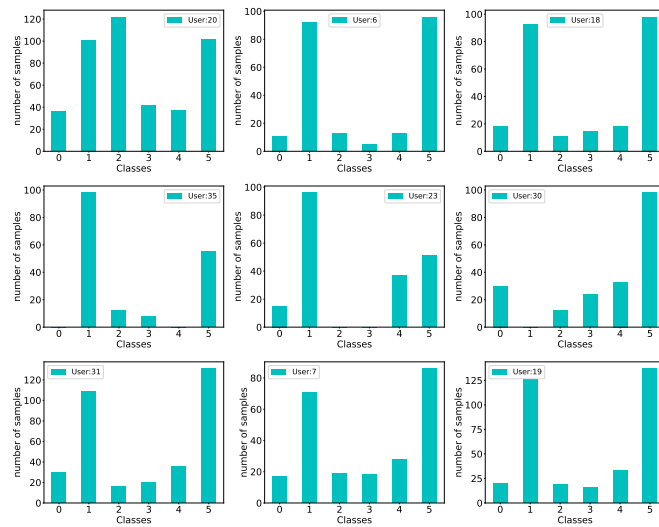
- [20] Mingsheng Long, Zhangjie Cao, Jianmin Wang, and Michael I. Jordan. Conditional adversarial domain adaptation. In *NeurIPS*, 2018.
- [21] Ian Goodfellow, Jean Pouget-Abadie, Mehdi Mirza, Bing Xu, David Warde-Farley, Sherjil Ozair, Aaron Courville, and Yoshua Bengio. Generative adversarial nets. In *Advances in Neural Information Processing Systems 27*, pages 2672–2680, 2014.
- [22] Mohamed Ragab, Zhenghua Chen, Min Wu, Haoliang Li, Chee-Keong Kwoh, Ruqiang Yan, and Xiaoli Li. Adversarial multiple-target domain adaptation for fault classification. *IEEE Transactions on Instrumentation and Measurement*, 70:1–11, 2020.
- [23] Qiao Liu and Hui Xue. Adversarial spectral kernel matching for unsupervised time series domain adaptation. In *Proceedings of the Thirtieth International Joint Conference on Artificial Intelligence, IJCAI-21*, 2021.
- [24] Mohamed Ragab, Zhenghua Chen, Min Wu, Haoliang Li, Chee-Keong Kwoh, Ruqiang Yan, and Xiaoli Li. Adversarial multiple-target domain adaptation for fault classification. *IEEE Transactions on Instrumentation and Measurement*, 70:1–11, 2020.
- [25] Jimpeng Li, Shuang Qiu, Changde Du, Yixin Wang, and Huiguang He. Domain adaptation for eeg emotion recognition based on latent representation similarity. *IEEE Transactions on Cognitive and Developmental Systems*, 12:344–353, 2020.
- [26] Sanjay Purushotham, Wilka Carvalho, Tanachat Nilanon, and Yan Liu. Variational recurrent adversarial deep domain adaptation. In *ICLR 2017: International Conference on Learning Representations 2017*, 2017.
- [27] Michele Tonutti, Emanuele Ruffaldi, Alessandro Cattaneo, and Carlo Alberto Avizzano. Robust and subject-independent driving manoeuvre anticipation through domain-adversarial recurrent neural networks. *Robotics and Autonomous Systems*, 115:162–173, 2019.
- [28] Kaichao You, Ximei Wang, Mingsheng Long, and Michael Jordan. Towards accurate model selection in deep unsupervised domain adaptation. In *International Conference on Machine Learning*, pages 7124–7133. PMLR, 2019.
- [29] Davide Anguita, Alessandro Ghio, Luca Oneto, Xavier Parra, and Jorge Luis Reyes-Ortiz. A public domain dataset for human activity recognition using smartphones. In *European Symposium on Artificial Neural Networks*, pages 437–442, 2013.
- [30] Jennifer R. Kwapisz, Gary M. Weiss, and Samuel A. Moore. Activity recognition using cell phone accelerometers. *Sigkdd Explorations*, 12(2):74–82, 2011.
- [31] Allan Stisen, Henrik Blunck, Sourav Bhattacharya, Thor Siiger Prentow, Mikkel Baun Kjærgaard, Anind Dey, Tobias Sonne, and Mads Møller Jensen. Smart devices are different: Assessing and mitigating mobile sensing heterogeneities for activity recognition. In *Proceedings of the 13th ACM Conference on Embedded Networked Sensor Systems*, pages 127–140, 2015.
- [32] Ary L. Goldberger, Luis A. N. Amaral, Leon Glass, Jeffrey M. Hausdorff, Plamen Ch. Ivanov, Roger G. Mark, Joseph E. Mietus, George B. Moody, Chung-Kang Peng, and H. Eugene Stanley. Physiobank, physiotoolkit, and physionet components of a new research resource for complex physiologic signals. *Circulation*, 101(23):215–220, 2000.
- [33] Emadeldeen Eldele, Zhenghua Chen, Chengyu Liu, Min Wu, Chee-Keong Kwoh, Xiaoli Li, and Cuntai Guan. An attention-based deep learning approach for sleep stage classification with single-channel eeg. *IEEE Transactions on Neural Systems and Rehabilitation Engineering*, 2021.
- [34] Markus Thill, Wolfgang Konen, and Thomas Bäck. Time series encodings with temporal convolutional networks. In *International Conference on Bioinspired Methods and Their Applications*, pages 161–173. Springer, 2020.
- [35] Shaojie Bai, J Zico Kolter, and Vladlen Koltun. An empirical evaluation of generic convolutional and recurrent networks for sequence modeling. *arXiv preprint arXiv:1803.01271*, 2018.
- [36] Kaiming He, Xiangyu Zhang, Shaoqing Ren, and Jian Sun. Deep residual learning for image recognition. In *2016 IEEE Conference on Computer Vision and Pattern Recognition (CVPR)*, pages 770–778, 2016.
- [37] Sicheng Zhao, Xiangyu Yue, Shanghang Zhang, Bo Li, Han Zhao, Bichen Wu, Ravi Krishna, Joseph E Gonzalez, Alberto L Sangiovanni-Vincentelli, Sanjit A Seshia, et al. A review of single-source deep unsupervised visual domain adaptation. *IEEE Transactions on Neural Networks and Learning Systems*, 2020.
- [38] Yaroslav Ganin, Evgeniya Ustinova, Hana Ajakan, Pascal Germain, Hugo Larochelle, François Laviolette, Mario Marchand, and Victor Lempitsky. Domain-adversarial training of neural networks. *JMLR*, 17(1):1–35, 2016.
- [39] Rui Shu, Hung Bui, Hirokazu Narui, and Stefano Ermon. A dirt-t approach to unsupervised domain adaptation. In *International Conference on Learning Representations*, 2018.
- [40] Arthur Gretton, Karsten M. Borgwardt, Malte J. Rasch, Bernhard Schölkopf, and Alexander Smola. A kernel two-sample test. *Journal of Machine Learning Research*, 13(1):723–773, 2012.
- [41] Mohammad Mahfujur Rahman, Clinton Fookes, Mahsa Baktashmotlagh, and Sridha Sridharan. On minimum discrepancy estimation for deep domain adaptation. *Domain Adaptation for Visual Understanding*, 2020.
- [42] Baochen Sun, Jiashi Feng, and Kate Saenko. Correlation alignment for unsupervised domain adaptation. In *Domain Adaptation in Computer Vision Applications*, pages 153–171. Springer, 2017.
- [43] Kuniaki Saito, Yoshitaka Ushiku, and Tatsuya Harada. Asymmetric tri-training for unsupervised domain adaptation. In *ICML’17 Proceedings of the 34th International Conference on Machine Learning*, pages 2988–2997, 2017.
- [44] Philipp Probst, Anne-Laure Boulesteix, and Bernd Bischl. Tunability: importance of hyperparameters of machine learning algorithms. *The Journal of Machine Learning Research*, 20(1):1934–1965, 2019.

A CLASS DISTRIBUTION OF DIFFERENT SUBJECTS

In this section, we visualize the class distribution of each selected subjects for all the datasets. Fig. S4(a) shows the classes distribution of subjects in UCIHAR dataset, where we notice that all subjects have data for all the classes. Counterpart, some subjects in WISDM dataset do not have data for some subjects as shown in Fig. S4(b).



(a) UCIHAR dataset



(b) WISDM dataset

Fig. 4. Class distribution of selected subjects among different datasets

B HYPER-PARAMETER IMPORTANCE

The importance of each hyper-parameter can be valuable when we have low budget for hyper-parameter tuning. As such, we can tune the most important hyper-parameter while fixing others to a specific value. In this section, we study how the different hyper-parameters can affect the model performance. Specifically, we test the learning rate against other model specific performance on three different domain adaptation algorithms. To do so, we leverage random forest model and feed the corresponding hyper-parameters as input and the target metric as output [44]. In our case, we averaged all the model selection risks and use them as metrics to calculate the importance of each parameter.

In Fig. 5, we study the effect of learning rate, the weights of the domain alignment loss in the UDA algorithm (differs according to the method), and the source classification loss \mathcal{L}_{cls} . We calculate the importance of these parameters while running the sweeps of three different methods i.e., DDC, Deep-CORAL and AdvSKM. The results reveal that the learning rate is the most significant parameter especially with SSC dataset, as it contributes with more than 80% of the performance. We conclude that more effort should be put in finding the best learning rate that suites each dataset. In addition, we find that the source classification loss comes next in the importance, and hence, more weight should be assigned to it.

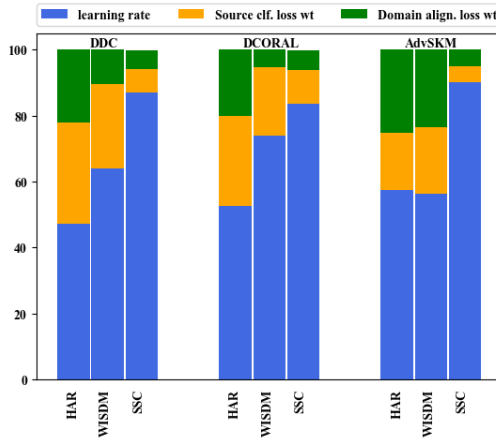


Fig. 5. Parameters importance for some selected UDA methods through the three datasets.

C DETAILED PARAMETER RANGES FOR THE HYPER-PARAMETER SEARCH

In Section III-G3, we described the way we selected the hyper-parameters for each UDA method. Here, we provide the detailed ranges for each parameter among all selected domain adaptation methods as shown in Table 5. For all the UDA algorithms, we tuned the learning rate from the range mentioned in the first row. For the next rows, we show the ranges for each specific loss in the prospective UDA method.

Table 5. Details of hyper-parameter tuning setup.

Method	Hyperparameter	Range
	Learning Rate	10^{-2} to 10^1
DDC	MMD loss	10^{-2} to 10^1
	Classification loss	10^{-1} to 10^1
Deep CORAL	Coral loss	10^{-2} to 10^1
	Classification loss	10^{-1} to 10^1
HoMM	High-order-MMD loss	10^{-2} to 10^1
	Classification loss	10^{-1} to 10^1
MMDA	MMD loss	10^{-2} to 10^1
	Coral Loss	10^{-2} to 10^1
	Conditional loss	10^{-2} to 10^1
	Classification loss	10^{-1} to 10^1
DSAN	Local MMD loss	10^{-2} to 10^1
	Classification loss	10^{-2} to 10^1
DANN	MMD loss	10^{-2} to 10^1
	Classification loss	10^{-1} to 10^1
CDAN	Adversarial loss	10^{-2} to 10^1
	Conditional loss	10^{-2} to 10^1
	classification loss	10^{-1} to 10^1
DIRT-T	Adversarial loss	10^{-2} to 10^1
	Conditional loss	10^{-2} to 10^1
	virtual adversarial	10^{-2} to 10^1
	Discriminator steps	10^{-2} to 10^1
	classification loss	10^{-1} to 10^1
CODATS	Adversarial loss	10^{-2} to 10^1
	classification loss	10^{-1} to 10^1
AdvSKM	Adversarial MMD loss	10^{-2} to 10^1
	Classification loss	10^{-1} to 10^1

D BACKBONE NETWORK ARCHITECTURE

We describe the detailed structure of the 1D-CNN network that we used as a backbone in ADA_{TIME} throughout our experiments, as illustrated in Fig. 6. It consists of 3-block CNN, and each block have a 1D convolutional layer, followed by a 1D batchNorm layer and a ReLU function for non-linearity and finally a 1D MaxPooling layer. The first convolutional layer in the first block have a kernel size of ϕ_k and a stride ϕ_s , and those differ according to the dataset. The details of their values for each dataset can be found on the Github repository.

Regarding to 1D-ResNet-18, we deployed the one mentioned in [36], which is now a standard architecture.

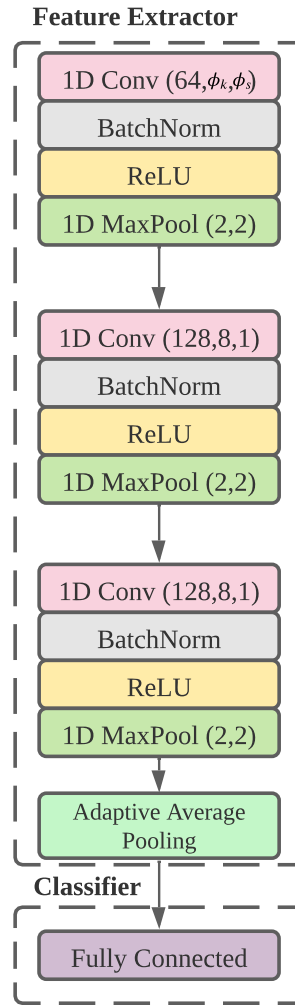


Fig. 6. Backbone network of 1D-CNN, where ϕ_k is the kernel size and ϕ_s is the stride.

E DETAILED RESULTS OF OUR FRAMEWORK

In this subsection, we provide the detailed results of the different risks experiments. In specific, Tables 6, 7, and 8, 9 show the mean and the standard deviation for each cross-domain scenario in UCIHAR, WISDM, SSC, and HHAR dataset respectively.

Table 6. Detailed results of scenarios of UCIHAR dataset in terms of MF1 score.

Risk	Algorithm	0→11	12→16	9→18	6→23	7→13	AVG
Target	DDC	60.00±13.32	66.77±8.46	61.41±5.80	88.55±1.42	77.29±2.11	75.67
	Deep-Coral	67.2±13.67	64.58±8.72	54.38±9.69	89.66±2.54	90.46±2.96	77.71
	HoMM	83.54±2.99	63.45±2.07	71.25±4.42	94.97±2.49	91.41±1.33	84.10
	MMDA	72.91±2.78	74.64±2.88	62.62±2.63	91.14±0.46	90.61±2.00	81.40
	DSAN	99.23±1.09	65.71±2.92	89.69±7.44	97.82±1.54	94.33±0.00	90.96
	DANN	98.09±1.68	62.08±1.69	70.7±11.36	85.6±15.71	93.33±0.00	84.97
	CDAN	98.19±1.57	61.20±3.27	71.3±14.64	96.73±0.00	93.33±0.00	86.79
	DIRT-T	98.13±2.64	82.05±8.61	85.90±6.63	93.76±3.10	93.35±0.00	92.20
	CoDATS	86.65±4.28	61.03±2.33	80.51±8.47	92.08±4.39	92.61±0.51	85.47
	AdvSKM	65.74±2.69	60.52±1.99	53.25±5.19	79.63±8.52	88.89±3.12	74.67
Few-shot	DDC	67.95±7.51	58.58±1.55	48.33±4.06	84.34±5.22	86.33±2.19	74.25
	Deep-Coral	70.86±5.85	59.3±0.77	58.5±10.7	89.5±1.6	85.23±3.01	77.23
	HoMM	78.87±8.37	60.34±1.07	66.97±3.41	93.84±2.04	87.82±4.43	81.3
	MMDA	74.36±9.26	66.01±5.15	54.92±4.27	95.88±1.2	93.33±0.0	79.54
	DSAN	89.47±8.76	65.97±2.59	78.02±7.52	96.68±2.74	92.61±0.51	87.13
	DANN	87.73±5.29	60.33±1.9	69.69±9.83	89.88±6.34	93.33±0.0	83.10
	CDAN	98.19±1.57	61.2±3.27	71.31±14.64	96.73±0.0	93.33±0.0	86.79
	DIRT-T	92.33±1.49	71.63±6.64	86.87±0.39	86.71±14.17	93.33±0.0	88.47
	CoDATS	71.6±15.34	65.1±0.68	64.51±14.12	92.04±4.05	81.41±6.04	79.10
	AdvSKM	64.45±2.59	61.99±4.07	53.13±4.59	78.09±9.92	88.89±3.12	74.47
DEV	DDC	72.0±3.51	59.65±4.11	45.42±5.89	86.14±1.97	81.66±8.07	74.14
	Deep-Coral	67.55±11.65	62.13±7.74	47.77±2.84	72.44±13.45	78.7±18.24	71.43
	HoMM	73.38±7.34	59.84±1.43	60.02±11.83	90.48±0.8	85.94±2.52	78.28
	MMDA	83.22±3.46	62.64±10.42	58.43±2.55	96.73±0.0	94.12±1.11	80.12
	DSAN	75.58±9.18	61.71±1.75	67.1±4.61	93.22±2.49	88.82±3.08	81.07
	DANN	77.77±18.26	63.26±2.49	57.49±7.77	95.86±1.84	91.71±0.84	80.89
	CDAN	71.51±8.84	54.66±2.91	40.94±3.18	61.31±9.02	82.06±11.91	64.66
	DIRT-T	88.44±9.23	58.47±2.98	65.89±13.25	90.56±8.73	93.73±0.56	82.54
	CoDATS	51.81±4.67	54.81±2.76	31.83±8.89	81.23±4.07	80.98±13.74	65.12
	AdvSKM	65.74±2.69	60.09±1.4	53.7±4.61	79.31±8.95	88.89±3.12	74.62
Source	DDC	53.28±5.44	64.59±6.34	41.99±1.47	89.01±2.14	85.65±7.92	68.83
	Deep-Coral	62.42±1.97	62.19±4.68	31.4±7.7	88.42±1.01	87.84±2.78	71.99
	HoMM	62.95±20.6	59.82±0.4	53.14±4.71	90.04±4.45	89.59±4.01	75.86
	MMDA	83.22±3.46	62.64±10.42	58.43±2.55	96.73±0.0	94.12±1.11	80.12
	DSAN	84.81±13.2	62.91±0.39	77.63±0.94	81.91±23.31	92.97±0.51	83.31
	DANN	70.28±2.86	65.45±4.76	71.34±6.17	90.0±2.71	90.51±0.86	79.82
	CDAN	88.73±4.7	60.25±4.61	81.39±6.15	96.73±0.0	92.97±0.51	86.55
	DIRT-T	88.44±9.23	61.36±2.41	78.88±4.12	98.64±1.39	93.01±0.46	86.72
	CoDATS	71.45±12.93	61.98±2.88	72.11±4.98	96.12±0.86	78.92±12.71	79.05
	AdvSKM	69.97±3.68	53.73±11.04	35.46±8.02	85.73±6.11	82.29±4.67	71.08

Table 7. Detailed results of scenarios of WISDM dataset in terms of MF1 score.

Risk	Algorithm	35→31	7→18	20→30	6→19	18→23	AVG
Target	DDC	51.84±5.68	43.56±0.66	65.83±2.04	62.58±2.72	51.36±10.81	55.03
	Deep Coral	56.48±8.18	44.32±1.79	66.33±2.17	63.11±3.17	56.91±3.24	57.43
	HoMM	58.49±7.79	53.64±3.48	70.94±2.8	74.88±6.55	56.96±24.07	62.98
	MMDA	54.37±5.23	47.75±2.04	66.35±2.1	76.68±5.71	74.7±2.28	63.97
	DSAN	70.35±1.44	44.77±4.4	69.53±4.91	49.85±7.48	65.88±7.21	60.08
	DANN	62.53±6.97	43.55±2.06	53.96±3.03	79.05±15.62	49.96±5.83	57.81
	CDAN	60.93±8.6	58.98±5.36	60.43±11.19	59.61±0.89	49.3±1.05	57.85
	DIRT-T	68.59±10.7	73.57±9.09	72.06±8.6	50.14±7.43	67.03±2.41	66.28
	CODATS	50.93±5.46	51.21±5.66	67.28±3.2	65.24±3.68	49.1±10.92	56.75
	AdvSKM	55.15±9.56	52.36±2.73	72.83±3.69	58.64±4.33	63.78±10.2	60.55
Few-shot	DDC	38.86±14.69	43.3±1.8	56.56±0.93	62.43±7.42	49.11±0.23	50.05
	Deep Coral	39.37±15.11	45.62±4.25	56.86±0.72	56.46±5.43	48.95±0.19	49.45
	HoMM	35.41±13.8	30.52±3.6	60.99±1.1	54.74±7.85	51.15±7.39	46.56
	MMDA	43.47±4.95	57.9±1.84	55.9±2.97	59.8±8.45	43.52±8.41	52.12
	DSAN	52.92±14.31	51.98±4.93	64.35±3.78	49.26±7.09	48.51±8.15	53.41
	DANN	43.11±9.84	43.08±1.21	57.63±2.53	55.2±4.93	48.23±0.4	49.45
	CDAN	54.53±1.31	57.03±0.53	64.55±6.06	39.76±7.63	47.85±0.46	52.75
	DIRT-T	62.52±10.06	68.8±7.94	62.31±5.49	51.86±6.68	67.56±0.51	62.61
	CODATS	40.68±24.05	37.82±2.61	61.01±1.2	56.3±8.87	47.38±1.23	48.64
	AdvSKM	57.43±12.5	73.58±1.33	71.2±3.2	78.28±3.05	67.78±0.79	49.02
DEV	DDC	48.85±16.15	45.17±6.65	70.04±10.28	57.51±6.89	42.4±8.53	52.80
	DeepCoral	42.36±11.34	47.07±7.25	67.16±4.86	65.06±3.76	47.57±8.73	53.85
	HoMM	66.29±0.84	48.67±6.31	65.3±2.45	63.78±4.35	62.11±7.57	61.23
	MMDA	60.34±7.52	41.58±8.79	64.39±4.28	55.74±3.88	64.47±10.75	57.30
	DSAN	57.25±6.07	52.77±2.23	63.4±0.7	53.35±5.37	55.76±1.46	56.51
	DANN	52.21±1.09	41.16±6.62	71.96±10.1	59.09±3.57	48.0±0.9	54.48
	CDAN	49.02±4.2	57.65±0.18	65.5±0.61	44.03±0.81	50.16±0.44	53.27
	DIRT-T	46.75±3.54	57.89±0.15	65.49±0.62	45.16±0.0	50.9±0.4	53.24
	CODATS	40.96±19.0	42.0±3.75	69.65±7.6	70.59±12.51	48.15±15.11	54.27
	AdvSKM	61.91±6.95	49.84±5.31	69.35±1.38	54.89±4.14	51.3±10.33	57.46
Source	DDC	51.47±5.69	43.65±0.78	65.83±2.04	62.58±2.72	51.36±10.81	54.98
	Deep Coral	53.46±7.12	43.65±0.78	66.08±2.05	63.16±3.14	51.36±10.81	55.54
	HoMM	57.94±7.0	43.23±0.53	65.47±1.13	63.91±4.12	56.91±3.24	57.49
	MMDA	61.44±6.08	49.79±6.76	67.82±1.37	60.83±0.27	47.78±5.98	57.53
	DSAN	57.25±6.07	52.77±2.23	63.4±0.7	53.35±5.37	55.76±1.46	56.51
	DANN	46.56±11.92	44.04±2.61	68.13±1.27	54.41±4.61	52.92±2.86	53.21
	CDAN	44.25±6.84	57.44±7.58	63.67±0.63	47.81±5.88	49.27±0.12	52.49
	DIRT-T	72.59±4.03	57.74±0.06	53.47±2.17	60.91±0.38	57.46±8.41	60.43
	CODATS	74.06±4.77	35.8±0.78	54.21±4.5	45.54±1.33	54.0±13.2	52.72
	AdvSKM	42.3±16.63	53.66±5.72	62.59±2.7	60.37±0.81	50.84±2.66	53.95

Table 8. Detailed results of scenarios of SSC dataset in terms of MF1 score.

Risk	Algorithm	16→1	9→14	12→5	7→18	0→11	AVG
Target	DDC	55.47±1.72	63.57±1.43	55.43±2.75	67.46±1.45	54.17±1.79	59.22
	Deep-Coral	55.50±1.74	63.50±1.36	55.35±2.64	67.49±1.50	53.76±1.89	59.12
	HoMM	55.51±1.79	63.49±1.14	55.46±2.71	67.50±1.50	53.37±2.47	59.06
	MMDA	62.92±0.96	71.04±2.39	65.84±1.08	70.95±0.82	43.23±4.31	62.79
	DSAN	59.87±2.84	70.71±2.79	65.55±0.79	68.44±1.39	38.28±3.57	60.57
	DANN	58.68±3.29	64.29±1.08	64.65±1.83	69.54±3.00	44.13±5.84	60.26
	CDAN	59.65±4.96	64.18±6.37	64.43±1.17	67.61±3.55	39.38±3.28	59.04
	DIRT-T	61.31±4.23	66.39±4.86	66.95±1.72	70.51±0.89	33.05±2.49	59.42
	CoDATS	63.84±3.36	63.51±6.92	52.54±5.94	66.06±2.48	46.28±5.99	58.44
	AdvSKM	57.83±1.42	64.76±3.0	55.73±1.42	67.58±3.64	55.2±4.19	60.21
Few-shot	DDC	55.48±1.76	63.54±1.33	55.32±2.94	67.5±1.5	54.28±1.68	59.22
	Deep-Coral	55.5±1.84	63.55±1.33	55.42±2.66	67.53±1.54	52.1±2.85	58.82
	HoMM	55.51±1.79	63.5±1.14	55.46±2.71	67.5±1.5	53.37±2.47	59.06
	MMDA	65.63±0.67	65.92±4.44	57.99±6.43	71.5±0.97	28.9±3.78	57.98
	DSAN	56.39±0.67	63.85±0.63	62.47±2.6	68.92±1.67	43.25±2.76	58.97
	DANN	58.68±3.3	64.3±1.08	64.65±1.83	69.54±3.0	44.13±5.84	60.26
	CDAN	59.87±2.67	63.55±3.16	62.13±1.8	64.12±0.48	31.19±8.26	56.17
	DIRT-T	56.33±5.86	65.15±1.99	64.88±5.58	69.83±1.57	34.99±0.54	58.23
	CoDATS	59.84±0.64	53.02±4.53	57.58±1.75	55.12±3.55	47.64±2.4	54.64
	AdvSKM	57.68±0.79	64.31±2.93	55.29±2.58	67.22±3.9	55.16±4.39	59.93
DEV	DDC	55.53±1.87	63.57±1.26	55.35±2.73	67.46±1.55	54.14±1.7	59.21
	Deep-Coral	55.5±1.84	63.55±1.33	55.42±2.66	67.5±1.5	52.1±2.85	58.81
	HoMM	55.57±2.0	63.66±1.48	55.87±2.93	67.49±1.51	50.93±4.31	58.70
	MMDA	63.44±1.49	67.14±4.78	64.93±1.21	71.89±1.44	39.88±4.96	61.49
	DSAN	58.76±2.02	69.45±4.04	64.92±1.65	68.69±0.99	37.43±2.9	59.85
	DANN	58.78±4.76	64.61±0.93	65.47±0.95	68.88±2.81	31.13±1.74	57.77
	CDAN	60.95±1.13	60.54±10.01	65.0±1.34	67.02±1.13	30.79±10.69	56.86
	DIRT-T	54.42±12.46	71.33±3.72	64.99±4.98	69.94±0.43	35.62±3.79	59.26
	CoDATS	60.03±1.18	52.22±10.55	56.96±2.4	68.64±2.93	41.1±5.14	55.79
	AdvSKM	57.8±0.69	64.27±2.93	55.12±2.52	67.31±3.83	55.11±4.56	59.92
Source	DDC	55.48±1.76	63.57±1.29	55.16±2.76	67.5±1.5	54.24±1.79	59.18
	Deep-Coral	55.5±1.74	63.5±1.36	55.35±2.64	67.5±1.5	53.76±1.89	59.12
	HoMM	55.51±1.79	63.5±1.14	55.46±2.71	67.5±1.5	53.37±2.47	59.06
	MMDA	59.6±0.51	68.25±4.17	65.63±0.85	71.06±0.99	45.89±1.97	62.08
	DSAN	63.05±3.14	63.84±10.11	57.55±11.16	68.84±2.25	37.46±4.76	58.14
	DANN	58.68±3.3	64.3±1.08	64.65±1.83	69.54±3.0	44.13±5.84	60.26
	CDAN	62.06±0.91	63.32±5.02	48.8±1.02	63.46±1.18	36.86±8.23	54.89
	DIRT-T	59.11±3.24	65.08±1.42	65.5±4.92	67.27±1.58	35.29±2.92	58.44
	CoDATS	56.52±1.76	68.2±5.72	59.72±6.66	63.31±3.9	36.05±8.95	56.76
	AdvSKM	57.78±0.72	64.29±2.97	55.15±2.52	67.33±3.82	55.16±4.4	59.94

Table 9. Detailed results of scenarios of HHAR dataset in terms of MF1 score.

Risk	Algorithm	0→6	1→6	2→7	3→8	4→5	AVG
Target	DDC	51.22±14.18	85.11±7.11	48.6±5.66	77.43±2.47	86.97±1.85	69.87±0
	Deep-Coral	57.64±4.59	89.81±0.33	44.15±0.92	79.3±0.3	90.53±3.05	72.28±0
	HoMM	64.85±0.96	89.12±0.61	44.44±0.6	80.2±1.1	88.73±3.01	73.47±0
	MMDA	61.66±4.66	90.85±0.51	53.36±8.87	88.07±5.29	91.24±4.96	77.04±0
	DSAN	56.47±10.89	92.77±1.03	61.07±1.46	98.14±0.51	97.26±0.47	81.14±0
	DANN	47.02±0.57	93.02±1.9	49.06±8.38	95.77±1.91	97.24±0.51	76.42±0
	CDAN	56.52±8.35	92.4±0.76	50.76±6.24	93.09±9.94	97.67±0.48	78.09±0
	DIRT-T	64.5±9.4	94.84±1.52	59.9±13.38	83.26±2.25	97.73±0.47	80.04±0
	CoDATS	46.45±0.64	92.59±0.71	48.13±8.96	96.89±1.97	96.38±2.42	76.09±0
	ADVSKM	59.39±4.59	81.43±5.52	47.75±3.98	79.05±0.42	82.03±3.24	69.93±0
Few-shot	DDC	61.61±1.95	78.86±14.46	47.77±4.89	78.4±1.31	79.65±3.13	69.26±0
	Deep-Coral	59.35±4.8	86.58±6.14	44.8±2.79	77.65±2.23	85.04±6.2	70.68±0
	HoMM	54.97±5.29	84.99±9.19	41.65±1.86	78.38±1.9	83.12±9.49	68.62±0
	MMDA	60.13±6.66	84.15±10.34	55.47±4.41	80.31±10.76	75.26±4.33	71.07±0
	DSAN	52.92±16.13	92.67±1.39	50.85±10.21	97.11±0.39	97.33±0.84	78.18±0
	DANN	53.84±6.34	86.38±12.08	57.48±1.61	78.94±6.82	91.78±8.26	73.68±0
	CDAN	45.52±0.9	92.99±0.7	54.1±7.12	98.17±0.37	96.39±1.37	77.43±0
	DIRT-T	54.88±15.6	94.05±1.3	64.63±0.3	80.6±0.45	97.9±0.68	78.41±0
	CoDATS	44.72±5.1	93.61±0.7	53.33±7.71	93.52±1.67	88.51±6.23	74.74±0
	ADVSKM	56.25±7.15	82.68±3.1	45.91±5.88	76.62±5.49	83.84±2.96	69.06±0
DEV	DDC	62.61±1.32	73.99±9.45	43.61±0.89	76.24±2.53	75.17±5.66	66.32±0
	Deep-Coral	54.82±9.16	89.31±1.44	48.44±1.98	77.39±2.81	79.44±4.64	69.88±0
	HoMM	63.58±2.24	88.49±2	47.12±4.27	79.23±1.13	84.07±1.19	72.5±0
	MMDA	59.52±3.77	86.53±2.06	48.99±10.42	77.8±2.28	78.3±7.36	70.22±0
	DSAN	58.81±7.19	93.42±0.64	45.61±0.5	98.44±0.23	98.47±0.32	78.95±0
	DANN	46.54±0.61	90.73±1.97	46.58±3.13	83.43±10.12	95.83±0.28	72.62±0
	CDAN	45.52±0.9	92.99±0.7	54.1±7.12	98.17±0.37	96.39±1.37	77.43±0
	DIRT-T	52.63±9.77	93.1±2.06	63.49±1.95	87.08±10.06	97.13±0.44	78.69±0
	CoDATS	44.7±1.65	91.98±1.01	47.56±5.04	91.83±4.56	92.52±3.14	73.72±0
	ADVSKM	45.52±0.9	92.99±0.7	54.1±7.12	98.17±0.37	96.39±1.37	77.43±0
Source	DDC	62.18±1.56	79.2±9.5	44.53±1.32	76.65±1.83	75.53±4.9	67.62±0
	Deep-Coral	63.14±1.57	88.27±3.02	44.59±0.43	78.33±1.77	79.55±2.64	70.78±0
	HoMM	63.14±2.11	87.58±2.59	47.27±4.92	77.62±1.67	80.28±0.56	71.18±0
	MMDA	65.42±1.48	69.07±1.49	41.67±0.96	76.62±3.05	78.2±6.97	66.2±0
	DSAN	56.42±8.91	93±0.54	49.68±7.7	84.28±12.64	97.53±0.3	76.18±0
	DANN	61.04±3.52	91.78±0.61	53.44±2.85	80.95±1.68	94±1.88	76.24±0
	CDAN	45.52±0.9	92.99±0.7	54.1±7.12	98.17±0.37	96.39±1.37	77.43±0
	DIRT-T	47.26±0.16	94.06±0.81	57.55±9.64	81.14±0.15	97.78±0.78	75.56±0
	CoDATS	52.32±9.64	93.36±0.11	43.67±0.86	91.06±11.21	95.16±2.16	75.11±0
	ADVSKM	56.08±2.45	76.28±8.67	38.54±9.01	79.73±1.33	82.29±5.25	66.58±0